Black Carbon Impact on Snow and Vegetation Interactions Affecting Environmental Feedback Loops and Climate Change

Gladimir V. G. Baranoski*, Petri M. Varsa and Hong Guan

Natural Phenomena Simulation Group, School of Computer Science, University of Waterloo,
200 University Avenue West, Waterloo, Ontario, N2L 3G1, Canada

ABSTRACT

Snow and vegetation interactions are being significantly affected by global warming conditions, particularly in high altitude and high latitude regions. The increase in vegetation productivity (greening) observed in these snowy regions has become one the main drivers of feedback loops leading to the intensification of climate change. Concomitantly, the spectral quality of photosynthetically active radiation (PAR) propagated by snow covers can be affected by their black carbon (BC) contents. The resulting variations in the red to blue, red to far-red and blue to far-red spectral ratios of propagated PAR can potentially influence a number of fundamental photobiological phenomena associated with the growth and development of plants above and underneath snowpacks. Consequently, these variations may contribute to vegetation changes that can reinforce feedback loops. Despite the importance of these interconnected biophysical processes, an evidence-based understanding about BC-elicited variations in the spectral quality of PAR reflected and transmitted by snow is still lacking. In this paper, we address this knowledge gap by methodically evaluating the sensitivity of snow reflectance and transmittance to varying amounts of BC impurities, and examining their impact on the corresponding spectral ratios. Our investigation is conducted using an *in silico* approach supported by measured data obtained from natural snow samples with distinct characteristics. Our findings unveil specific qualitative and quantitative trends for BC-elicited variations in the spectral ratios of PAR propagated by snow. Besides advancing the current knowledge about photobiological phenomena with serious environmental ramifications, our investigation also highlights practical aspects relevant for the effective prediction and management of such ramifications, notably through the combined use of remote sensing technologies, *in situ* experiments and high-fidelity simulations. Furthermore, it is expected that the employed *in silico* experimental framework can also serve as a reliable platform for future environmental studies involving the effects of BC impurities on snow radiometric responses.

Keywords: snow, carbon-based impurities, photosynthetically active radiation, reflectance, transmittance, spectral ratios, vegetation greening, feedback loops.

1. INTRODUCTION

The importance of snow for the sustainability of life on Earth has been widely recognized. Besides representing a vital source of freshwater[1–3] and providing essential thermal insulation for different biomes,[4–6] it also has a strong influence on radiative forcing processes affecting the planet's climate.[7–9] Moreover, the snow light attenuation mechanisms associated with these processes can affect both the quantity and quality (spectral distribution) of photosynthetic active radiation (PAR) propagated to the vegetation present in snowy regions,[10,11] eliciting photobiological responses that can further alter the ecology and energy balance of these regions.[12–14] Not surprisingly, snow cover variations have a central role in a broad scope of environmental studies.[1,2,6,9,14–17]

In the last decades, the deposition of light-absorbing impurities (LAIs)[18] into snow, notably those originating from anthropogenic activities, has also been brought to the forefront of interdisciplinary research initiatives involving climate change.[7,8,19,20] This can be attributed to the scientific community's increasing interest in the feedback loops associated with global warming[16,17,21] as well as in the compounding effects that the deposition of these impurities in snow-covered landscapes can have on the viability of local ecosystems and in the accentuation of those loops.[9,22] Despite recent advances in these intertwined areas of research, the impact that the deposition of LAI particles can have on the photobiological interactions between snow and vegetation has yet to be fully unravelled along with its far-reaching environmental ramifications.

*Corresponding author's email address: gvgbaran@uwaterloo.ca.

Remote Sensing for Agriculture, Ecosystems, and Hydrology XXVII, edited by Christopher M. U. Neale, Antonino Maltese, Charles R. Bostater, Alexandre Castagna, Proc. of SPIE Vol. 13666, 136660W
2025 Published by SPIE · 0277-786X · doi: 10.1117/12.3072417

Small particles of LAI base materials, such as carbon and dust, can be wind transported far from their sources and reach snow-covered regions across the planet.[9,23,24] Once these aerosols, also referred to as light-absorbing particles (LAPs),[8] are deposited in a snowpack, they can alter its light attenuation mechanisms. More specifically, they can enhance light absorption, notably in the visible (photosynthetic) spectral domain. This, in turn, leads to a reflectance (albedo) decrease and heating. The latter accelerates the growth of snow grains, which further decreases reflectance, and increases snowmelt. The surface darkening resulting from the decrease of snowpack reflectance and the exposure of materials (*e.g.*, soil and vegetation) underneath it further increase the energy available for melting.[8,20,25]

Besides these radiative forcing processes associated with variations in the amount of light absorbed within the contaminated snowpacks, there are also effects associated with light propagated (reflected and transmitted) by them and impinging on the nearby vegetation. The resulting changes in vegetation productivity, or greening,[11,15,16,26] are also known to affect radiation exchange and snowmelt.[3] These interconnected processes can substantially contribute to the aforementioned feedback loops[16,21] and, consequently, have a significant impact on the local an global climate.[7–9,18,22]

In this work, we primarily address the effects of carbon-based impurities, also referred to as light-absorbing carbon (LAC) particles,[23,27] on the spectral quality of light reflected and transmitted by snow. It is worth noting that the deposition of LAC particles in snow is less episodic than that of dust particles.[18] Moreover, the effects of both types of particles are comparable even though the LAC concentrations in snow are often on the order of parts per *billion*, while the concentrations of dust particles are often on the order of parts per *thousand* (by mass).[18,22] This aspect underscores the stronger absorption efficiency of the former.

The LAC particles can be loosely divided into two main groups, namely black (inorganic) and brown (organic) carbon.[28,29] As previously noted,[27,29] the term "black carbon" (BC) has been employed inconsistently in the related literature. Within the context of this work, it refers to carbonaceous materials that are formed during the incomplete combustion of fossil fuels (*e.g.*, motor vehicle aerosols) and strongly absorb light across the entire visible spectral domain. On the other hand, brown carbon (BrC) refers to carbonaceous materials that are associated with biomass burning (*e.g.*, wood smoke aerosols) and absorb light primarily at low visible wavelengths.[8,28,29] Although both BC and BrC have been shown to be key climate forcing parameters whose influence on the planet's energy budget needs to be properly accounted for,[29–31] this investigation focus on the former due to its dominant light-absorbing role, ubiquity and more established optical properties.[8,22,23,28]

It has been extensively demonstrated that PAR markedly affects a wide range of photobiological responses affecting the growth and physiological development of plants, from seed germination and chlorophyll production to stem elongation and photoperiodism.[12,32,33] The extent of its impact on different types vegetation and on the equilibrium of their hosting biomes depends not only on the amount of light propagated (reflected and transmitted) in the photosynthetic domain, but also on its spectral quality.[34–36] This can be quantified in terms of red (600-700 nm) to blue (400-500 nm), red to far-red (700-800 nm) and blue to far-red ratios of propagated light, denoted by R/B, R/FR and B/FR, respectively.[33,34]

In the case of seed germination, the breaking of dormancy for many species, including those found in high altitude or high latitude regions, is induced by variations in the R/FR ratios.[13,32] It is also believed that spectral variations in solar light play a pivotal role in the regulation of the growing season and phenology of vegetation found in those regions.[37,38] For instance, trees located at latitudes above the Arctic polar circle need to induce growth cessation and bud formation even during periods that they are exposed to light, *i.e.*, without an actual expression of photoperiodism.[39] The net effect of these two phenomena is commonly referred to as bud set,[40] a complex physiological process representing the transition phase from active growth to dormancy.[41] It has been speculated that this process is enhanced by increases in the R/FR ratios of light impinging on the trees.[13,39] It has also been noted that the inhibition of stem elongation prompted by increases in R/FR ratio of light reaching Arctic trees is also regulated by the amount of available blue light.[13]

Given the significant effects of BC impurities on the attenuation of light in the photosynthetic domain, it is likely that their presence could alter the spectral ratios of PAR propagated by snow covers. Such alterations, in turn, would result in observable changes in the productivity of different types of vegetation found in snowy regions. Despite the importance that such changes may have for the ecology and climate of those regions, existing

studies in this area usually do not specifically address the effects of BC impurities on the quality of light reflected and transmitted by snow.[17,20] Among the main obstacles faced by research efforts aimed at this timely topic, one can highlight the difficulties that the low concentration of BC impurities deposited in snowpacks can pose for the detection and analysis of their impact on snow spectral responses.[42]

Due to these difficulties, Warren[19] recommended the use of computer modeling in conjunction with controlled laboratory experiments on artificial snow with large amounts of BC impurities.[7] We note, however, that artificially prepared snow samples often lack the morphological diversity (*e.g.*, different grain sizes and shapes) found in natural samples. Moreover, the use of large amounts of BC impurities may defeat the purpose of studies specifically attempting to determine BC-induced effects on the light propagation mechanisms of snowpacks located in high altitude and high latitude regions of interest for climate studies. These snowpacks are often characterized by the presence of relatively small, albeit influential, amounts of these carbon-based materials.[19,20,43,44]

To overcome the constraints outlined above, we employed a computational (*in silico*) investigation approach to assess the sensitivity of the spectral ratios of PAR reflected and transmitted by snow samples containing realistic amounts (within ranges reported in the related literature) of BC impurities. More specifically, we conducted controlled *in silico* experiments, supported by nivological and radiometric data obtained from real snowpacks, using the model for light and snow interactions known as SPLITSnow (*SP*ectral *LI*ght *T*ransport in *Snow*).[45,46] This first-principles model explicitly accounts for the particulate nature of snow in order to output reliable radiometric data (*e.g.*, spectral reflectance and transmittance) for different experimental scenarios. In addition, as described in the next section section, its original ray-optics formulation has been expanded to predictively simulate light attenuation effects elicited by the presence of carbon-based impurities deposited in dry and wet snow samples through suspension and sedimentation processes.

Our investigation findings are expected to strengthen the current knowledge about the interactions among light, snow, BC impurities and vegetation. Such an evidence-based understanding is essential for the reliable interpretation of *in situ* and remote observations of biomes severely affected by global warning[15,22] and, consequently, for the implementation of more effective procedures for the monitoring and management of those biomes. Moreover, it provides the foundation for the development of more comprehensive climate change models that can appropriately take into consideration not only vegetation greening and feedback loops prompted by variations in PAR reflected and transmitted by pure and BC-contaminated snow,[9,21] but also the long-term ecological implications of these processes. These include, but are not limited to, the expansion and reduction of vegetation covers in snowy regions more susceptible to increasing warming conditions such as the Arctic.[15,17]

The remainder of this paper is organized as follows. In Section 2, we describe the algorithmic features incorporated into the core component of our *in silico* experimental framework. In Section 3, we outline the data and the methodology employed in our investigation. In Section 4, we present our findings. In Section 5, we discuss their significance for environmental and climate studies involving snow and vegetation interactions affected by the presence of BC impurities. We then conclude in Section 6 with a summary of the outcomes of our investigation and directions for future research in this area.

2. LIGHT ATTENUATION BY CARBON-BASED IMPURITIES

The *in silico* experimental framework employed in this investigation has as its central component the SPLITSnow model.[45] The ray-optics formulation of this stochastic model allows for a (light) ray interacting with a given snow sample to be associated with any wavelength (denoted by λ) within the spectral domain of interest. In this section, we present the algorithmic features specifically incorporated into the model to account for the presence of BC and BrC impurities.

As indicated in the SPLITSnow's formulation,[45,46] the probability of a ray being absorbed while traversing an ice grain can be calculated using the following equation based on the Beer-Lambert law:[47,48]

$$p_{a_g}(\lambda) = 1 - e^{-\alpha_{ice}(\lambda) d_g}, \tag{1}$$

where $\alpha_{ice}(\lambda)$ and d_g correspond to the specific absorption coefficient (*s.a.c.*) of ice and the distance travelled within a grain, respectively.[45]

Similarly, the probability of a ray being absorbed while traversing pore space occupied by liquid water can be expressed as:

$$p_{a_p}(\lambda) = 1 - e^{-\alpha_{water}(\lambda) d_p}, \tag{2}$$

where $\alpha_{water}(\lambda)$ and d_p correspond to the *s.a.c.* of water and the distance travelled within the pore space, respectively.[45]

The *s.a.c.* of ice can be expressed as:

$$\alpha_{ice}(\lambda) = \frac{4\,\pi\,k_{ice}(\lambda)}{\lambda}, \tag{3}$$

where $k_{ice}(\lambda)$ corresponds to the imaginary part of the complex refractive index of ice.[49] To obtain the *s.a.c.* of water, the term $k_{ice}(\lambda)$ in Eq. 3 is replaced by $k_{water}(\lambda)$, the imaginary part of the complex refractive index of water.[50,51]

We note that, depending on the length unit selected for d_g and d_p (*e.g.*, cm), λ in the right side of Eq. 3 has to be converted to the reciprocal, or inverse, of that unit (*e.g.*, cm^{-1}). In this way, $\alpha_{ice}(\lambda)$ and $\alpha_{water}(\lambda)$ are also given in that reciprocal unit, and the probability p_a becomes unitless, varying from 0 to 1 as expected.

In order to account for the occurrence of BC and BrC impurities in the ice grains (through a sedimentation process[30]) and/or in the pore space (through a suspension process[43]), we employ a more comprehensive version of Eq. 1. More precisely, the probability of absorption of a ray traversing a given grain is computed using the following equation:

$$p_{a_g}(\lambda) = 1 - e^{-(\alpha_{ice}(\lambda) + \alpha_{BC}(\lambda) S_{BC} + \alpha_{BrC}(\lambda) S_{BrC}) d_g}, \tag{4}$$

where $\alpha_{BC}(\lambda)$ and $\alpha_{BrC}(\lambda)$ correspond to the *s.a.c.* of BC and BrC impurities, respectively, and the parameters S_{BC} and S_{BrC} (ranging from 0 to 1) represent the fractions of these materials present in the grains through sedimentation.

Likewise, the probability of absorption of a ray traversing a portion of the pore space containing liquid water as well as suspended BC and BrC impurities is computed using the following equation:

$$p_{a_p}(\lambda) = 1 - e^{-(\alpha_{water}(\lambda) + \alpha_{BC}(\lambda)(1-S_{BC}) + \alpha_{BrC}(\lambda)(1-S_{BrC})) d_p}. \tag{5}$$

We also employ Eq. 5 when the traversed portion of the pore space does not contain water. However, in this case, the term $\alpha_{water}(\lambda)$ is set to zero.

The *s.a.c.* of BC impurities is computed using the following formula derived from related works[28,29,52,53] on the light absorption by these materials:

$$\alpha_{BC}(\lambda) = \frac{\mathcal{M}_{BC}\ \lambda_{BC}}{\lambda^{\mathcal{A}_{BC}}} c_{BC}\, D, \tag{6}$$

where $\mathcal{M}_{BC}$, $\mathcal{A}_{BC}$ and c_{BC} correspond to the mass absorption efficiency[22,28,53] (or MAE, in m^2/g), the Angstrom exponent[54,55] and the concentration (in ng/g) of the BC impurities, respectively, while λ_{BC} is the reference wavelength (in nm) used to experimentally obtain $\mathcal{M}_{BC}$[54,55] and D represents the density of the snow sample (in kg/m^3).

Both D and c_{BC} in Eq. 6 refer to the sample in a dry state. However, if the employed c_{BC} value refers to the sample in a wet state, *i.e.*, with a water saturation (fraction of the pore space occupied by liquid water, denoted by $S \in [0..1]$) greater than zero, then D in Eq. 6 is replaced by:[46]

$$D_{wet} = D + S\, D_{water} \left(1 - \frac{D}{D_{ice}}\right), \tag{7}$$

where D_{water} and D_{ice} correspond to the densities of pure liquid water and ice, respectively.

For the computation of the *s.a.c.* of BrC impurities, the terms referring to BC impurities in Eq. 6 are replaced by the corresponding terms referring to the former. It also worth mentioning that, since the MAE is commonly expressed in m^2/g, while D and the distances (d_g and d_p) may be expressed in kg/m^3 and cm, respectively, a conversion of units may be required so that $\alpha_{BC}(\lambda)$ and $\alpha_{BrC}(\lambda)$ are expressed in cm^{-1}.

3. MATERIALS AND METHODS

3.1 Snow Characterization Data

Within the employed *in silico* experimental framework, snow grains are described as prolate spheroids with a semi-major axis equal to b and a semi-minor axis related to b by the grains' sphericity ($\Psi \in [0..1]$, with Ψ equal to 1 yielding perfectly spherical grains),[45] which is represented by a random variable with a probability distribution previously employed for particulate materials.[45] As suggested in the UNESCO-IHP report on *The International Classification for Seasonal Snow on the Ground*, the "size of a grain or particle is its greatest extension".[56] Accordingly, in our simulations, the size of a grain corresponds to $2b$, with b also represented by a random variable. Similarly, the grains' facetness ($f \in [0..1]$, with f equal to zero yielding perfectly smooth grains) is represented by a random variable with a normal probability distribution.[45]

In studies involving simulations of snow spectral responses, one may choose to employ a representative virtual snow sample with a characterization primarily based on the assignment of average values (provided in the related literature) to the material parameters. In this investigation, to broaden our observations, we considered three representative virtual snow samples with distinct morphological traits, default BC contents and wetness levels. More precisely, we considered two dry samples (D1 and D2) associated with dry snowpacks formed on the Norwegian Svalbard archipelago in the Arctic,[57] and one wet sample (W) associated with a wet snowpack formed at the US Army Cold Regions Research and Engineering Laboratory in Hanover, USA.[10]

The descriptions and corresponding radiometric datasets for the dry snowpacks were provided by Salvatori *et al.*[57] and made available through the SISpec (Snow and Ice Spectral) library. These SISpec snowpack samples, identified as S158 and S197, were used to guide the selection of appropriate values (presented in Table 1) for the parameters employed in the characterization of samples D1 and D2, respectively. For the wet snowpack, identified here as P18 (assessed by Perovich on January 18), its description and radiometric data[10] were used to guide the characterization (Table 1) of sample W. For more details about the selection of parameter values used in the characterization of samples D1, D2 and W, the interested reader is referred to Appendix A.

Table 1: Parameter values employed in the characterization of the selected snow samples.

	Samples		
Parameters	D1	D2	W
Grain size range (μm)	150–450	400–1000	500–1000
Temperature ($^{\circ}C$)	-5	-1	-1
Thickness (cm)	11	19	11
Water saturation	0	0	0.18
Density (kg/m^3)	385	300	300
BC content (ng/g)	3	6	5
BC sedimentation fraction	1	1	0.5
Facetness range	0.01–0.23	0.2–0.4	0.1–0.3
Facetness mean	0.1	0.3	0.2
Facetness standard deviation	0.05	0.1	0.1
Sphericity range	0.6–0.95	0.6–0.95	0.7–0.95
Sphericity mean	0.9	0.8	0.85
Sphericity standard deviation	0.1	0.07	0.1

3.2 Black Carbon Properties

It has been recognized that different methodologies can be employed to obtain appropriate values for the parameters used to quantify the absorptive properties of BC impurities,[53,54] namely, the reference wavelength λ_{BC}, the mass absorption efficiency $\mathcal{M}_{BC}$ and the Angstrom exponent $\mathcal{A}_{BC}$ introduced earlier (Section 2). In this work, the selection of values for these parameters was based on the aethalometer method.[54] This choice took into account the widespread use of this method and the fact that it does not depend on supplemental data sources.[54,58]

Accordingly, we set λ_{BC} to 880 nm, which corresponds to the standard wavelength employed in BC measurements using aethalometers since the absorption of light by other compounds, notably BrC impurities, at this wavelength is markedly weaker than that at lower wavelengths.[58] Thus, the aethalometer readings are unlikely to be biased by the possible concomitant presence of BrC compounds in the material sample employed in BC measurements.

Similarly, we set $\mathcal{M}_{BC}$ to 16.619 m^2/g, which corresponds to the value recommended by the manufacturer of these devices when they operate at 880 nm.[59] Hence, the product $\mathcal{M}_{BC}\,\lambda_{BC}$ becomes equal to 14625, a value consistently employed by related works in this area.[29–31,55,59] Lastly, we elected to set $\mathcal{A}_{BC}$ to 1 as the default value for the Angstrom exponent of BC impurities as indicated by relevant studies involving the light absorption by these aerosols.[28,29,54]

3.3 In Silico Experimental Setup

Our controlled *in silico* experiments consisted primarily in the computation of directional-hemispherical reflectance and transmittance curves for the selected snow samples using the SPLITSnow model,[45] with its formulation expanded to account for the presence of carbon-based impurities as previously described (Section 2). These curves were computed considering a spectral resolution of 5 nm, with 10^6 incident rays per sampled λ. This number of rays was selected to ensure asymptotically convergent radiometric readings with a confidence of 0.1% as indicated by the exponential Chebyshev inequality.[48] Regarding the light incidence geometry, we considered a normal angle of incidence of 0° (with respect to the samples' normal vector). As reported below, this choice took into account the measured conditions in which the reference radiometric datasets were obtained.

The measured reflectance curves[57] correspond to reflectance factors calculated considering a hemispherical incidence geometry, with an acquisition sensor positioned directly above the target snowpacks. The modeled reflectance curves, on the other hand, correspond to directional-hemispherical reflectances. We note that in studies involving the radiometric responses of materials characterized by a near-Lambertian behaviour, such as snow irradiated from an angle of incidence of 0°,[60] for practical purposes directional-hemispherical reflectance and hemispherical-directional reflectance factor can be used interchangeably.[61]

As for the modeled transmittance curves, our *in silico* experimental setup was based on the experimental setup employed by Perovich.[10] More precisely, we computed the transmittance values at the indicated thickness (equivalent to the depth of the samples' bottom boundary). Thus, once a (light) ray exits a snow sample at the specified thickness (bottom depth), it is considered permanently propagated by the sample, *i.e.*, it no longer contributes to the sample's transmittance values at that depth. In the experimental setup employed by Perovich,[10] the transmittance acquisition sensor was placed on the top of a dark plywood platform, above which snow was accumulated following snowfalls. We also note that an angle of incidence of 0° allows for more light to penetrate the samples. This, in turn, yields not only stronger reflectance responses to BC contamination,[7] but also relatively larger and, thus, more dependable transmittance responses[11,61,62]

Our *in silico* experiments were organized into three stages. Initially, in stage I, we compared modeled radiometric curves computed for the selected samples with measured radiometric curves obtained for the reference snowpacks.[10,57] This enabled us to verify the plausibility of the samples' characterization datasets (Table 1) and to establish well-grounded baselines for our subsequent experiments. Afterwards, in stages II and III, we conducted reflectance and transmittance experiments to assess the respective impact of BC content variations on the spectral ratios of PAR reflected and transmitted by the selected snow samples.

While, in stage I, we used the default values (Table 1) assigned to the BC contents (concentrations), in stages II and III, we considered incremental increases to those values. These increments were based on ranges provided in the related literature,[19,20,43,43,44] notably for snow deposits located in the Northern hemisphere. More specifically, for the reflectance experiments, we considered BC contents varying from zero to 36 ng/g, with increments of 9 ng/g. We note that the amount of light transmitted by snowpacks, even just a few cms thick, is significantly smaller than the amount of reflected light. Hence, in order to obtain transmittance values with a magnitude appropriate for the analysis of light transmission profiles, we employed a narrower range, from zero to 12 ng/g, and a smaller increment, 3 ng/g.

Finally, as generally acknowledged, two aspects are particularly essential for the dependability of any *in silico* investigation, namely, the assessment of its predictions' fidelity[63] and the means to enable their reproducibility and replicability.[64] We note that the predictive capabilities of the SPLITSnow model[45] employed in our experiments have been extensively evaluated through quantitative and qualitative comparisons with actual measured data and observations reported in the related literature.[11,46,65,66] Also, the degree of fidelity of its predictions was further illustrated through our stage I experiments described in Section 4.1. Regarding their reproducibility and replicability, it is worth mentioning that we made SPLITSnow accessible for online use[67] through our model distribution system.[68] Furthermore, all supporting datasets, such as the spectral refractive indices for water and ice, employed in this work are openly available in a dedicated data repository.[69]

3.4 Sensitivity Analysis

To complement our reflectance and transmittance experiments, we also carried out a differential sensitivity analysis[70,71] with respect to the impact of increasing BC content on the samples radiometric responses across the blue (400-500 nm), green (500-600 nm), red (600-700 nm) and far-red (700-800 nm) bands of the spectral domain of interest. For this analysis, we employed a sensitivity index (SI) that provides the rate of the change in the output quantities, which correspond to snow reflectance and transmittance in this work, to the change in a selected snow characterization parameter while the other parameters are kept fixed.[71] A rate equal to 1.0 indicates complete sensitivity (or maximum impact), while a rate less than 0.01 indicates that the output quantity is insensitive to changes in the selected parameter.[72]

Relying on these concepts, we computed the mean sensitivity index (MSI) for the four selected spectral bands. This allowed us to quantify the mean rate of change in reflectance and transmittance with respect to alterations in BC content, within these bands. More specifically, for the reflectance curves, this index is expressed as:

$$MSI = \frac{1}{N}\sum_{i=1}^{N} SI_i = \frac{1}{N}\sum_{i=1}^{N} \frac{|\rho_c(\lambda_i) - \rho_e(\lambda_i)|}{\max\{\rho_c(\lambda_i), \rho_e(\lambda_i)\}}, \tag{8}$$

where ρ_c and ρ_e correspond to the reflectance values computed for the control (without BC impurities) and examined cases, respectively, and N is the total number of wavelengths (λ_i) sampled with a 5 nm resolution within a selected spectral band. Similarly, for the transmittance curves, the ρ_c and ρ_e values in Eq. 8 are replaced by the control and examined transmittance values denoted by τ_c and τ_e, respectively.

3.5 Spectral Ratios

To examine the effects of increasing BC contents on the spectral quality of PAR propagated by the snow samples, the reflectance and transmittance experiments were accompanied by the calculation of the selected spectral ratios using the following formulas:[33,34]

$$R/B = \frac{\rho(660)}{\rho(400)}, \tag{9}$$

$$R/FR = \frac{\rho(660)}{\rho(730)}, \tag{10}$$

and

$$B/FR = \frac{\rho(400)}{\rho(730)}, \tag{11}$$

where $\rho(\lambda)$ denotes the reflectance value obtained at the wavelength λ (in nm).

Similarly, to quantify the spectral quality of the light transmitted by the samples, the $\rho(\lambda)$ values in Eqs. 9 to 11 were replaced by transmittance values denoted by $\tau(\lambda)$.

4. RESULTS

4.1 Stage I - Baseline Experiments

As shown in the graphs presented in Fig. 1, the radiometric curves computed for the virtual snow samples considered in this investigation showed a close agreement with the measured curves provided by Salvatori *et al.*[57] and Perovich[10] for the reference natural snowpacks (Section 3.1). In fact, the root-mean-square errors (RMSE) calculated for the modeled curves depicted in Fig. 1 were below 0.01 (or 1%). More precisely, the RMSE values obtained for samples D1 (Fig. 1a), D2 (Fig. 1b) and W (Fig. 1c) were equal to 0.0048, 0.0044 and 0.0021, respectively. This degree fidelity[63] enabled us to reliably proceed to the next stages of our investigation.

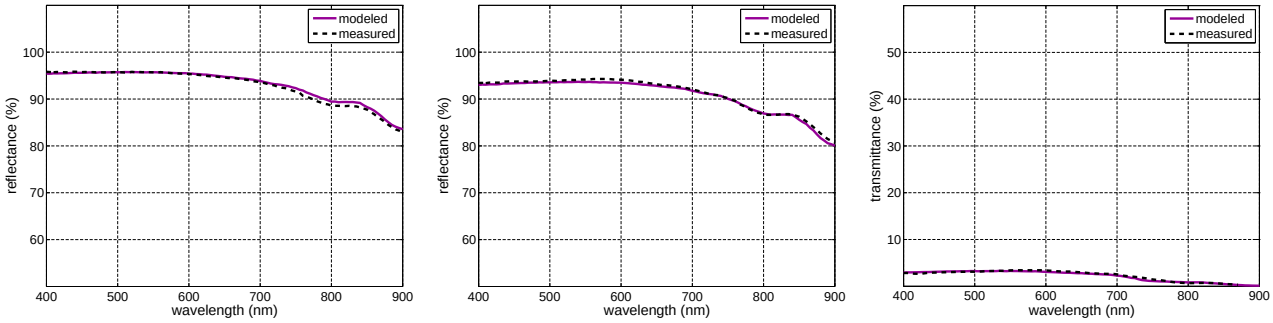

(a) (b) (c)

Figure 1: Comparison of modeled and measured radiometric curves. (a) Sample D1. (b) Sample D2. (c) Sample W. The modeled curves were computed using the SPLITSnow model and the snow characterization datasets presented in Table 1. The measured reflectance curves were provided by Salvatori *et al.*,[57] while the measured transmittance curve was provided by Perovich.[10]

4.2 Stage II - Reflectance Experiments

The reflectance curves obtained for the dry samples D1 (Fig. 2a) and D2 (Fig. 2b) depicted a nonlinear decrease following an increase in their BC contents. This trend is consistent with previous analytical and laboratory-based observations about the reflectance of BC-contaminated snow reported in the literature.[19,73] Although the same qualitative behaviour was also observed in reflectance curves obtained for the wet sample W (Fig. 2c), their overall magnitude was lower than that of the curves obtained for the dry samples. This quantitative aspect, in turn, is consistent with *in situ* observations about the reflectance reduction prompted by the presence of liquid water in the pore space of natural snowpacks.[10] We note that, in previous works involving the simulation of BC effects on the reflectance of snow samples, there was no specific indication of the presence of liquid water in their pore space.[7,74]

In Fig. 3, we provide the MSI plots computed for the BC-affected reflectance curves of each snow sample (Fig. 2). As shown in these plots, the impact of BC impurities monotonically increased across the spectral (PAR) domain of interest, with the largest and smallest MSI values being obtained for the blue and far-red bands, respectively. Furthermore, although the MSI values calculated for each spectral band increased as we considered larger BC content, the rate of change (ROC) associated with each band became less accentuated.

In Fig. 4, we present the spectral ratios of reflected light computed for the snow samples. While the B/FR and R/FR ratios decreased as we considered larger BC contents, the R/B ratios increased. The plots presented in Fig. 4 also show that the ROC was more accentuated for the B/FR ratio, followed by the R/B ratio and then the R/FR ratio. Furthermore, the ROCs observed for the B/FR and R/B ratios became less accentuated as the BC contents were increased. In the case of the R/FR ratio, although the ROC noticeably decreased for the initial BC content variations, from 0 to 18 ng/g, it exhibited a nearly linear behaviour for the subsequent BC content variations, from 18 to 36 ng/g. All these rends were observed for the three snow samples.

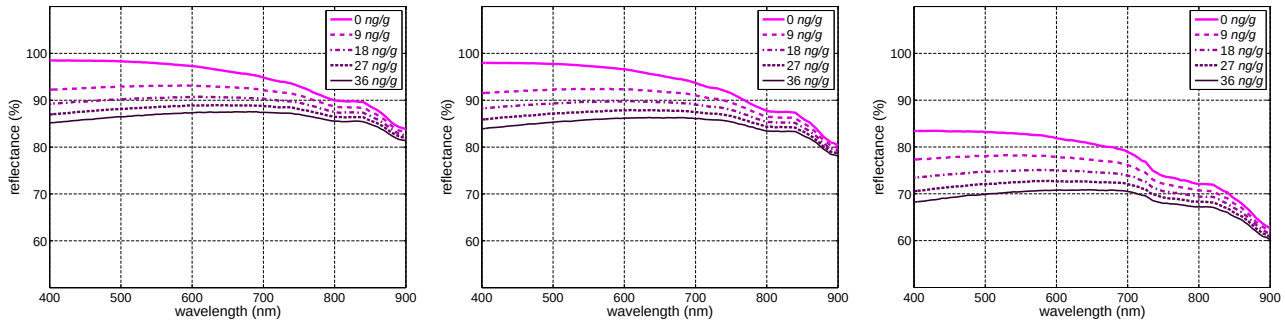

(a) (b) (c)

Figure 2: Modeled reflectance curves obtained considering incremental increases in the samples' BC contents. (a) Sample D1. (b) Sample D2. (c) Sample W. The curves were computed using the SPLITSnow model and the snow characterization datasets presented in Table 1 unless otherwise stated.

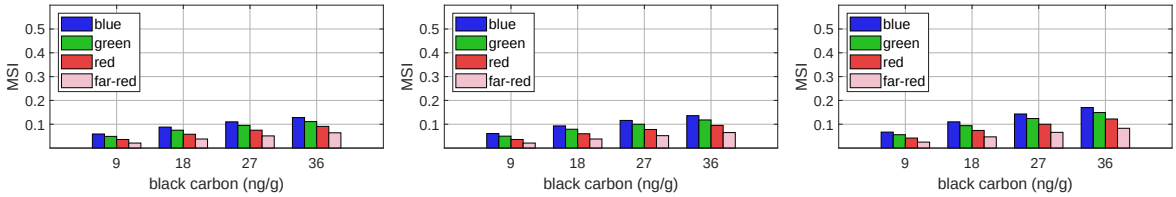

(a) (b) (c)

Figure 3: MSI values computed across the blue (400-500 nm), green (500-600 nm), red (600-700 nm) and far-red (700-800 nm) bands for the samples' modeled reflectance curves (Fig. 2) associated with increasing BC contents. (a) Sample D1. (b) Sample D2. (c) Sample W.

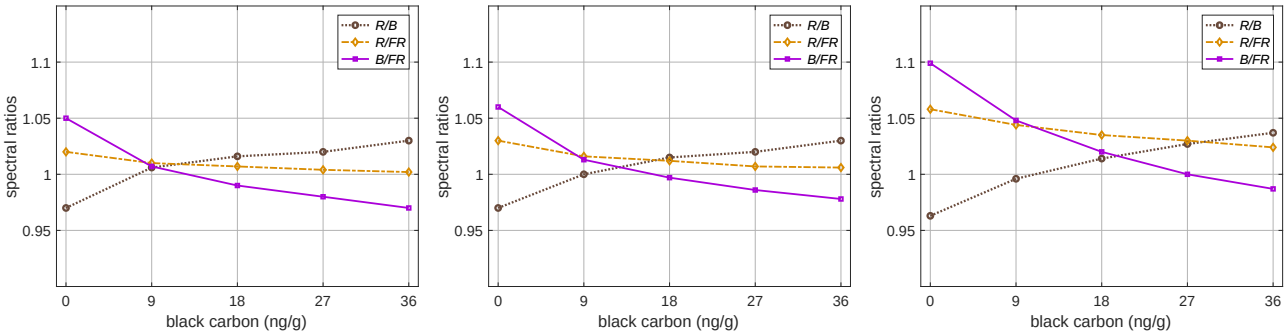

(a) (b) (c)

Figure 4: Spectral ratios calculated using the samples' reflectance values (Fig. 2) computed considering incremental increases in their BC contents. (a) Sample D1. (b) Sample D2. (c) Sample W.

As also indicated in Fig. 4, the computed spectral ratios of reflected light were characterized by a relatively small magnitude, with wider ranges being observed for the wet sample W (Fig. 4c). It is important to note, however, that even subtle changes in these ratios can significantly affect the plants' metabolism[37] and alter physiological processes associated with their adaptation to varying environmental conditions.[13]

4.3 Stage III - Transmittance Experiments

To the best of our knowledge, previous laboratory and computational studies involving BC effects on the propagation of light by snow have not addressed the impact of BC impurities on transmittance responses.[7,8,22,73–75] The scarcity of information in this area may be explained by the technical difficulties associated with the *in situ* measurement of these responses[10] as well as by the fact that usually light transport models for snow are primarily developed to output reflectance values.[74,76] Viewed in this context, the results of our *in silico* transmittance experiments, presented in Figs 5 to 7, can be seen as a fresh assessment of light transmission by BC contaminated snow, notably with respect to the spectral quality of the transmitted light.

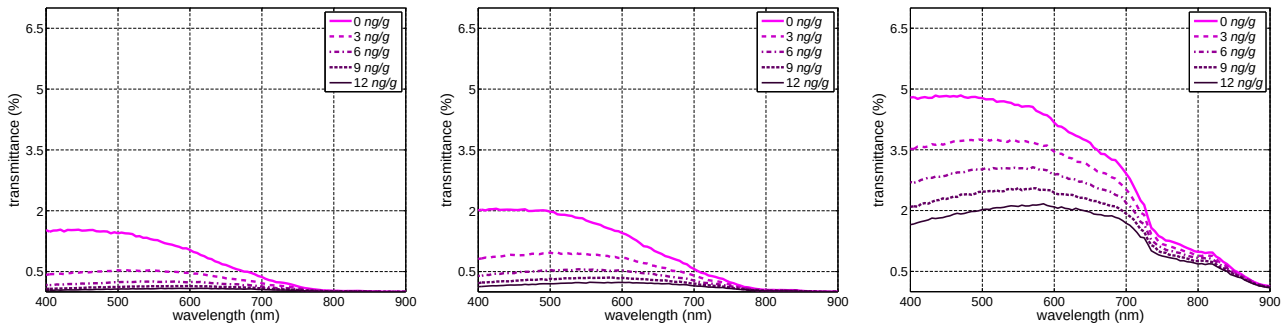

Figure 5: Modeled transmittance curves obtained considering incremental increases in the samples' BC contents. (a) Sample D1. (b) Sample D2. (c) Sample W. The curves were computed using the SPLITSnow model and the snow characterization datasets presented in Table 1 unless otherwise stated.

As shown in Fig. 5, the transmittance curves obtained for samples D1, D2 and W depicted a markedly nonlinear decrease following an incremental rise in their BC contents. Such a decrease is likely to be associated with the nonlinear light absorption properties of the BC impurities.[29] However, there may be other factors that need to be taken into account. For instance, in the case of wet sample W, while its reflectance curves were lower than the reflectance curves obtained for samples D1 and D2 (Fig. 2), its transmittance curves were higher than the transmittance curves computed for those samples (Fig. 5). This suggests that the presence of liquid water in its pore space can also have a noticeable effect in its light attenuation mechanisms. By reducing the refractive index differences between the snow (ice) grains and the surrounding medium, the presence of liquid water increases the probability of light being refracted from the grains to the pore space.[11] This sequence of events, in turn, may mitigate the attenuation of light transmitted through the sample.

In Fig. 6, we provide the MSI plots computed for the BC-affected transmittance curves of each snow sample (Fig. 5). In these plots, we can observe the same qualitative trends identified for the MSI values computed for the BC-affected reflectance curves (Fig. 3). In short, the impact of BC impurities monotonically increased across the spectral (PAR) domain of interest, with the largest and smallest MSI values being obtained for the blue and far-red bands, respectively. However, we noted a relevant quantitative difference. More precisely, the MSI values obtained for the transmittances were remarkably higher than those calculated for the reflectances. This aspect indicates that the transmitted light is distinctively more sensitive to the presence of BC impurities than the reflected light. It is also worth noting that this difference in sensitivity was lessened by the presence of liquid water in the pore space. More specifically, for the wet sample W, the MSI values obtained for the BC-affected reflectances (Fig. 3c) were relatively higher (compared to those obtained for the other samples), while the MSI values obtained for the BC-affected transmittances (Fig. 6c) were relatively lower (also compared to those obtained for the other samples).

In Fig. 7, we present the spectral ratios of transmitted light computed for the snow samples. Again, we can observe the same qualitative trends identified for the spectral ratios of reflected light (Fig. 4). Namely, while the B/FR and R/FR ratios decreased as we considered larger BC contents, with the former having a markedly more accentuated ROC, the R/B ratio increased. However, the obtained spectral ratios of transmitted light (Fig. 7) were remarkably higher than the spectral ratios of reflected light (Fig. 4). This observation is consistent with

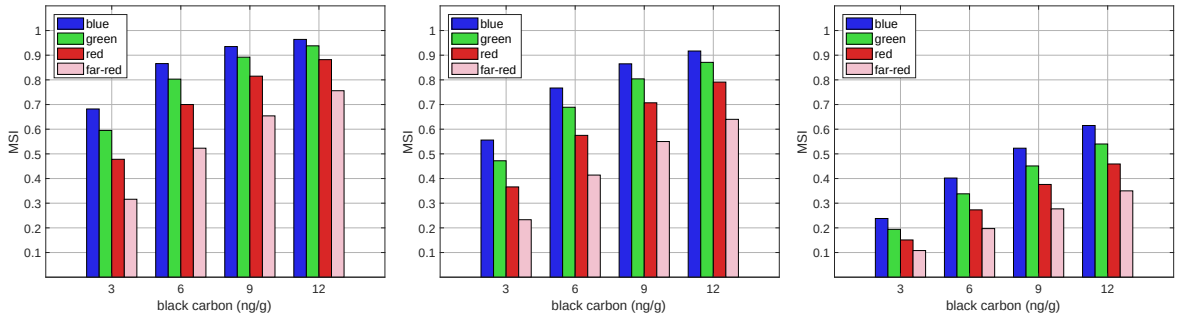

(a) (b) (c)

Figure 6: MSI values computed across the blue (400-500 nm), green (500-600 nm), red (600-700 nm) and far-red (700-800 nm) bands for the samples' modeled transmittance curves (Fig. 4) associated with increasing BC contents. (a) Sample D1. (b) Sample D2. (c) Sample W.

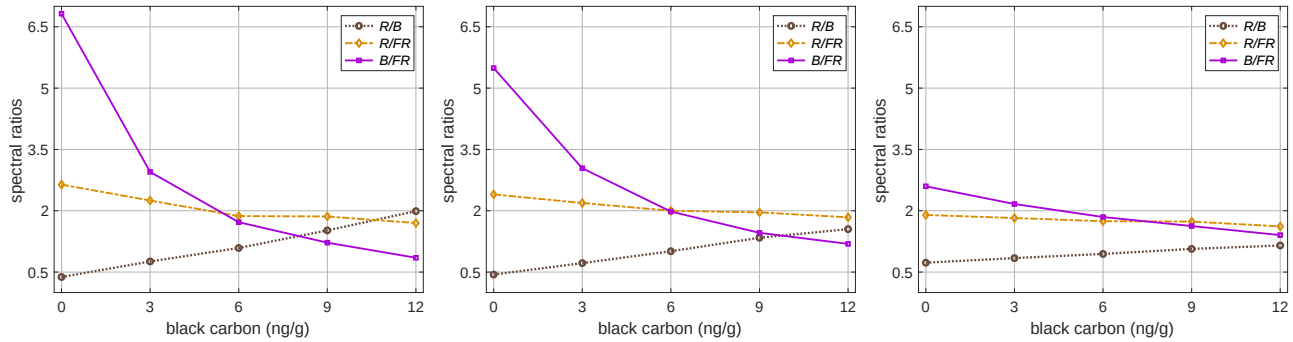

(a) (b) (c)

Figure 7: Spectral ratios calculated using the samples' transmittance values (Fig. 5) computed considering incremental increases in their BC contents. (a) Sample D1. (b) Sample D2. (c) Sample W.

the higher magnitude the MSI values calculated for the transmittance curves (Fig. 6) in comparison with those calculated for the reflectance curves (Fig. 3). Lastly, the wet sample W presented the least accentuated ROCs for all three spectral ratios (again, compared to those obtained for the other snow samples), further alluding to a mitigating effect elicited by the presence of liquid water in its pore space.

5. DISCUSSION

5.1 Vegetation Connections

The results of our *in silico* experiments presented in the previous section showed that the increase in the samples' BC contents led to the increase in their R/B ratios and the decrease in the R/FR and B/FR ratios calculated for both reflected and transmitted light. In the case of the spectral ratios of reflected light, their BC-elicited variations are more likely to affect the growth and physiological development of plants whose organs are completely or partially above a snow cover (*e.g.*, trees). It has been postulated that decreases in the R/FR ratio and reductions in amount of blue light (leading to higher R/B and lower B/FR ratios) impinging on these plants can inhibit their dormancy and promote stem elongation.[13,39] Accordingly, the variations in the spectral ratios of reflected light observed in our *in silico* experiments suggest that the increase in the BC contents of snow covers may promote the continuation of these plants' growth in periods in which they would normally transition to a dormant state.

In the case of the spectral ratios of transmitted light, although they can also positively affect the growth of plants whose organs may be partially covered by a relatively thin layer of cover, they are known to particularly

influence physiological processes directly associated with the different life stages of subnivean vegetation. For instance, it has been reported that seed germination and organ emergence can be inhibited by decreases in the R/FR ratios,[32,77] while cold tolerance activation and chlorophyll production can be inhibited by reductions in the amount of blue light (*i.e.*, higher R/B and lower B/FR ratios) reaching plants found completely below snow covers.[34,78] Thus, the variations in the spectral ratios of transmitted light observed in our *in silico* experiments, namely R/FR and B/FR decreases, and R/B increase, suggest that the increase in the BC contents of snow covers may negatively affect the growth and physiological development of subnivean vegetation.

Based on the observed *in silico* trends outlined earlier, one can draw preliminary inferences about the ecological effects of BC impurities deposited in snow covers. More specifically, it is possible that the presence of these impurities, even in relatively small amounts (below 40 ng/g), may inhibit the growth of graminoids (*e.g.*, herbaceous sedges[15]) and nonvascular plants (*e.g.*, mosses found in colder areas of Arctic tundra[17]) whose photosynthetic organs (located close the ground) are more likely to receive light transmitted by snow covers than light reflected by them. Conversely, it is also possible that the presence of BC impurities may promote the growth of vascular plants (*e.g.*, trees[39]) whose photosynthetic organs (located further away from the ground) are more likely to receive light reflected by snow covers than light transmitted by them.

These inferences align with reported evidence indicating the expansion of forested areas in high latitude regions[17,38] as well as the shift of Arctic tundra vegetation toward vascular plants,[79] namely shrubs, which are normally more dominant in relatively warmer areas.[17] Hence, it is probable that the net result of the aforementioned positive and negative effects of snow-deposited BC impurities on the physiological development of vascular and non-vascular plants may further contribute to the extensive vegetation greening verified in these biomes, which has been linked to increasing snowmelt and land warming conditions.[15,17,79]

As with any investigation centered on computer simulations, our *in silico* findings are subject to confirmation through comparisons with measured data to be obtained from controlled *in situ* experiments conducted on natural snow covers containing BC impurities, preferably located in regions of interest for climate change studies. We remark, however, that the intrinsic difficulties associated with *in situ* experiments[10,19] have been, and continue to be, key incentives for a myriad of computational (modeling) initiatives aiming at addressing the knowledge gaps in this area.[7,8,18,20,22,24,74]

5.2 Climate Connections

Besides the impact of vegetation greening on the ecology of biomes found in high altitude regions (*e.g.*, the Alps, the Andes, the Himalayas and the Rockies)[16,80] and high latitude regions (*e.g.*, the Arctic),[15,21,79,81] all of considerable relevance for global warming studies, it can also play a significant part in feedback loops that can dramatically affect the planet's climate.[17,21] For instance, it can alter solar energy exchanges that can lead to faster snowmelt and reduced snow cover. These, in turn, further intensify greening, which can potentially reduce the amount of melt water available for the plants during their growing stages.[3,16] As a consequence, at a certain point, vegetation productivity may start to decrease. In addition to impairing the biodiversity of the affected biomes,[21] this can prompt noticeable alterations in their host terrains' absorbed radiation profile and temperature regime, which represent physical quantities directly associated with environmental (soil-snow-vegetation-climate) feedback loops.[16,82]

The presence of BC impurities in snow and their effects in the spectral quality of light reaching the vegetation found in the affected regions can potentially shift the tipping point of vegetation productivity. We remark that our findings suggest that BC-elicited variations in the spectral ratios of light propagated by snow may promote greening in landscapes with a dominant presence of species that grow higher, and mitigate it in landscapes with a dominant presence of species that grow closer to the ground. Moreover, they also suggest that these processes may become more intense as the amount of deposited BC impurities increases. Such alterations in the type of vegetation coverage of a given region can result in changes in its surface albedo. As pointed by Yu *et al.*,[17] these changes could further affect the local climate and the planet's energy budget.[17]

It is also worth mentioning that a significant decrease in BC deposition, notably in the Northern Hemisphere, is projected for the next decades.[9] Such a decrease, would likely alter snow cover contributions to climate

changes.[20,22] In the case of the spectral quality of light propagated by snow with reduced levels of BC contamination, one would expect a corresponding reduction of the effects prompted by BC impurities. Nonetheless, the ever-evolving dynamics of these interconnected environmental processes[14,15,20] accentuates the need for their effective monitoring and predictive analysis.

5.3 Black Carbon Issues

Given the environmental ramifications of vegetation greening and its inferred sensitivity to variations in the amount of snow-deposited BC impurities, such variations need to be carefully evaluated. However, despite its importance, the precise quantification of BC impurities in snow-covered landscapes remains elusive, notably in regions more affected by global warning.[20,42,44]

Recall that the amount of BC impurities deposited in snow is relatively small in natural settings.[19] Accordingly, its effects on snow spectral responses can be markedly masked by alterations in other snow characteristics such as grain size.[11,20,42] Despite the current technological limitations in this area, the impact of BC impurities on snow spectral responses should not be overlooked. It can significantly influence the outcomes of highly specialized applications[14,15,17] involving the assessment of snow and vegetation interactions.

Previous studies involving the impact of BC impurities on light propagated by snowpacks[18,19,22,73,74] were primarily based on the analysis of snow reflectance responses. The results of our *in silico* experiments indicate that snow transmittance responses may be more sensitive to the BC impurities' light absorption efficiency than snow reflectance responses. Moreover, they suggest that the presence of liquid water in the pore space of snowpacks tends to mitigate this different level of sensitivity. Given their direct connections with the light penetration depth (at which incident light is reduced by $\geq 99\%$[11,83]) of snow layers covering important natural resources, such as vegetation and soil,[17] these transmittance related aspects should be also taken into account in future studies in this area.

6. CONCLUSION

In this paper, we have employed an *in silico* experimental approach supported by measured data to investigate the effects of BC impurities on the spectral quality of light propagated by snow. Our experimental results depicted similar qualitative and distinct quantitative trends for the BC-elicited variations in the spectral ratios of PAR reflected and transmitted by snow. More specifically, for both light propagation mechanisms, the R/B ratios increased while the R/FR and B/FR ratios decreased as we considered rising BC amounts (within ranges reported for natural snow deposits). These trends, however, were considerably more prominent for transmitted light. In fact, our findings indicate that snow transmittance is more sensitive to the presence of BC impurities than its reflectance. They also suggest that these differences tend to be mitigated by the presence of liquid water in the pore space of snowpacks.

A myriad of photobiological phenomena linked to plant growth and development, from seed germination to stem elongation, are prompted by variations in the spectral quality of PAR impinging on vegetation. The aforementioned BC-elicited trends for the spectral ratios of reflected and transmitted light are likely to positively affect the productivity of higher vegetation and negatively affect the productivity of subnivean vegetation, respectively. Accordingly, they may play a part in the expansion and retraction of different types of vegetation observed in regions of particular interest for the assessment of climate change processes such as the Arctic. Consequently, we believed that these trends need to be taken into account in the analysis and prediction of greening alterations leading to feedback loops with a direct impact on the ecological sustainability and energy budget of snow-covered biomes found in those regions.

The aspects mentioned above stress the importance of closely monitoring and studying the interactions between light, snow, BC impurities and vegetation, notably in high altitude and high latitude regions more affected by global warning conditions. Given the geographical location of these regions, the use of remote sensing technologies may be instrumental for the success of those initiatives. It has been noted in the literature, however, that the relatively small amounts of BC impurities deposited in natural snow covers pose considerable difficulties

for these technologies. It has also been acknowledged that, to overcome these difficulties, it is essential to strengthen the current understanding about the impact of these particles on the light attenuation mechanisms of snowpacks.

We aimed to align our investigation with these efforts by systematically examining the sensitivity of the spectral responses of distinct snow samples to changes in their BC content. It is worth noting that, to the best of our knowledge, no prior study has addressed the effects BC-contaminated snow deposits on the light propagated by other natural materials covered by them. Hence, the insights derived from our transmittance experiments bring forward aspects relevant for the remote sensing of a wide variety of landscapes, from forests to deserts.

The interconnected processes addressed in our investigation are highly complex, not only in terms of the sheer number of biophysical variables that need to be considered, but also with respect to their spatial and temporal scales. Accordingly, the investigation presented in this paper leads to a number of avenues for future research. These include, but are not limited to, the in-depth examination of the entangled effects of snow melting and the accumulation of BC impurities, as well as the comprehensive assessment of the impact of heterogenous distributions of these particles in multilayered snowpacks (*e.g.,* resulting from distinct snow falling events) on the dynamics of those processes and on the spectral responses of key remote sensing targets such as soil and vegetation. We note that such responses are central in the calculation of spectral indices, such as the NDVI (normalized difference vegetation index)[84] and the NDSI (normalized difference snow index),[85] extensively used in the remote sensing applications involving those targets.

We believe that new developments in these intertwined lines of research will rely on the pairing of good quality measured data obtained *in situ* and remotely, with reliable predictions obtained through high-fidelity computer simulations. The results of our *in silico* experiments also indicated, both quantitatively and qualitatively, that such predictions can be provided by the first-principles computational framework employed in this investigation, notably with respect to the effects of BC impurities on snow reflectance and transmittance. Accordingly, we expect that it can serve as an *in silico* platform not only to extend the scope of this study, but also to facilitate the interdisciplinary exploration of related timely topics, such as the coupling effects of greening and snowmelt alterations on the carbon uptake of vegetation under accentuated warming conditions, by the scientific community.

ACKNOWLEDGMENTS

This work was supported by the Natural Sciences and Engineering Research Council of Canada (NSERC-Discovery Grant 238337).

Appendix A: Selection of Parameter Values for the Virtual Snow Samples

As stated in Section 3.1, we used real snow samples, namely SISpec samples S158 and S197 as well as Perovich's sample P18, as references to *guide* the selection of parameter values used in the characterization of the virtual samples D1, D2 and W, respectively. In other words, whenever actual information and data were available, that information was taken into account. For example, general nivological information and snow profile diagrams were made available in the SISpec database alongside the measured reflectance curves for samples S158 and S197,[57] and a general description of sample P18 was provided by Perovich[10] alongside its measured transmittance curve. In this appendix, we briefly outline the steps (supported by the aforementioned quantitative information) leading to the assignment of values to the main snow characterization parameters listed in Table 1.

To select the parameter values used in the characterization of the virtual samples D1 and D2, we initially consulted the nivological information provided in the SISpec database for the respective SISpec samples as well as their snow profile diagrams. It is worth noting that some particular qualitative aspects needed to be considered for some parameters. For example, the thickness reported as general nivological information about a given sample corresponds to its top (uppermost) layer. However, for many SISpec samples, a close examination of their profile diagrams indicates that there are several additional layers of snow beneath the top layer. In several instances, this layer can have a dominant role associated with its specific morphological characteristics, with most of the relevant light attenuation processes taking place within it. These aspects were corroborated by the SISpec leading administrator.[86] Accordingly, they were also taken into account in the selection of thickness

values for the virtual samples, with more relevance being attributed to their top layers when appropriate (*e.g.*, relatively low amount of light transmitted to the bottom layers).

For the selection of the parameter values used in the characterization of the virtual sample D1, we elected to consider the top layer of the SISpec sample 158 since its characteristics allow for a negligible amount of light transmission to its bottom layers. This layer was composed of rounded grains and its reported thickness was 11 cm. Accordingly, we employed the same value for the thickness of sample D1, and selected a grain size range leading to a mean grain size equal to 300 μm, which corresponds to the grain size reported for the top layer of sample S158. In addition, the density and temperature of sample D1 were set to 385 kg/m^3 and -5°C, respectively, which also correspond to the measured values for the top layer of sample S158.

For the virtual sample D2, we elected to examine all layers of the SISpec sample S197 since its uppermost layer was only 1 cm thick, allowing for significant light transmission to the bottom layers. Accordingly, we set the thickness of sample D2 equal to 19 cm, which corresponds to the aggregated thickness of all layers of sample S197, which were mostly composed by rounded grains. Moreover, its thin top layer had particles with a relatively wide range of sizes, up to 1000 μm, its second layer was composed by particles with an average size equal to 1000 μm, while its third and fourth layers were composed by particles with average sizes equal to 500 μm. Thus, for sample D2, we assigned a grain size range, namely 400–1000 μm, that approximately encapsulated the most relevant grain sizes reported for sample S197. Since the density of the top layer of sample S197 was not provided, we chose to set the density of sample D2 to 300 kg/m^3, which is within the range of values provided for the densities of the second and third layers of sample S197. Regarding the temperature of sample D2, we elected to use the temperature of the top layer of sample S197, namely -1 °C.

For the virtual sample W, we used as reference the parameters values reported by Perovich[10] in his description of sample P18, which was composed of rounded grains. More precisely, for the thickness and grain size range of sample W, we assigned the values specified in Perovich's description, namely 11 cm and 400–1000 μm, respectively. For its density, we selected a value, 300 kg/m^3, that corresponds to the value associated with the middle portion of sample P18 as also reported by Perovich.[10] As for the temperature of sample W, based on Perovich's description of the metamorphic conditions of sample P18 (its actual temperature was not reported), we elected to set the temperature of virtual sample W to -1 °C, a value close to the snow freezing point.

Lastly, in the absence of supporting quantitative data for specific characterization parameters, such as water saturation and black carbon content, we considered qualitative information associated with the reference samples. For instance, while the SISpec samples were reported to be dry,[57,86] the Perovich's wet sample was reported to be "saturated in water".[10] Accordingly, for the virtual sample W, we selected a water saturation value ($S = 0.18$, which corresponds to a free water content of approximately 13% of the sample's total volume considering its density equal to 300 $kg\ m^{-3}$) consistent with wetness levels provided in the literature for snowpacks in similar conditions.[56] Also, the values (between 3 to 6 ng/g) assigned to the default BC contents of the virtual samples were selected taking into account BC content ranges reported for natural snowpacks[19,20,43] located in regions susceptible to levels of BC contamination similar to those affecting the provenance regions of the reference samples.

REFERENCES

[1] Barnett, T., Adam, J., and Lettenmaier, D., "Potential impacts of a warming climate on water availability in snow-dominated regions," *Nature* **438**(7066), 303 (2005).

[2] Cooper, E., Dullinger, S., and Semenchuk, P., "Late snowmelt delays plant development and results in lower reproductive success in high Arctic," *Plant Sci.* **180**, 157–167 (2011).

[3] Zheng, J., Jia, G., and Xu, X., "Earlier snowmelt predominates advanced spring vegetation greenup," *Agr. Forest Meteorol.* **315**, 1245:1–19 (2022).

[4] Beaglehole, D., Ramanathan, B., and Rumberg, J., "The UV to IR transmittance of Antarctic snow," *J. Geophys. Res.* **103**(D8), 8849–8857 (1998).

[5] Sanders-DeMott, R., McNellis, R., Jabouri, M., and Templer, P., "Snow depth, soil temperature and plant-herbivore interactions mediate plant response to climate change," *J. Ecol.* **106**, 1508–1519 (2018).

[6] Zhu, L., Ives, A., Zhang, C., Guo, Y., and Radeloff, V., "Climate change causes functionally colder winters for snow cover-dependent organisms," *Nat. Clim. Change* **9**, 886–893 (2019).
[7] Hadley, O. and Kirchstetter, T., "Black-carbon reduction of snow albedo," *Nat. Clim. Change* **2**, 437–440 (2012).
[8] Skiles, S., Flanner, M., Cook, J., Dumont, M., and Painter, T., "Radiative forcing by light-absorbing particles," *Nat. Clim. Change* **8**, 964–971 (2018).
[9] Hao, D., Bisht, G., Wang, H., Xu, D., Huang, H., Qian, Y., and Leung, L., "A cleaner snow future mitigates Northern hemisphere snowpack loss from warming," *Nat. Commun.* **14**, 6074:1–10 (2023).
[10] Perovich, D., "Light reflection and transmission by a temperate snow cover," *J. Glaciol.* **53**(181), 201–210 (2007).
[11] Baranoski, G. and Varsa, P., "Environmentally induced snow transmittance variations in the photosynthetic spectral domain: Photobiological implications for subnivean vegetation under climate warming conditions," *Remote Sens.* **16**(927), 1–23 (2024).
[12] Walker, D., Billings, W., and De Molenaar, J., "Snow-vegetation interactions in tundra environments," in [*Snow ecology: An interdisciplinary examination of snow covered ecosystems*], Walker, D., ed., 266–324, Cambridge University Press, Cambridge, UK (2001).
[13] Taulavuori, K., Sarala, M., and Taulavuori, E., "Growth responses of trees to Arctic light environment," in [*Progress in Botany 71*], Lüttge, U., Sarala, M., and Taulavuori, E., eds., 157–168, Springer-Verlag (2010).
[14] Pedersen, S., Liston, G., Ramstore, M., Abermann, J., Lund, M., and Schmidt, N., "Quantifying snow controls on vegetation greenness," *Ecosphere* **9**(6), e02309:1–21 (2018).
[15] Kim, J., Kim, Y., Zona, D., Oechel, W., Park, S., Lee, B., Yi, Y., Erb, A., and Schaaf, C., "Carbon response of tundra ecosystems to advancing greenup and snowmelt in Alaska," *Nature Com.* **12**, 6879:1–12 (2021).
[16] Rumpft, S., Gravery, M., Brönnimann, O., Luoto, M., Cianfrani, C., Mariethoz, G., and Guisan, A., "From white to green: Snow cover loss and increased vegetation productivity in the European Alps," *Science* **376**, 1119–1122 (2022).
[17] Yu, L., Leng, G., and Python, A., "Attribution of the spatial heterogeneity of Arctic surface albedo feedback to the dynamics of vegetation, snow and soil properties and their interactions," *Environ. Res. Lett.* **17**, 014036:1–13 (2022).
[18] Skiles, S. and Painter, T., "Daily evolution in dust and black carbon content, snow grain size, and snow albedo during snowmelt, Rocky Mountains, Colorado," *J. Glaciol.* **63**(237), 118–132 (2017).
[19] Warren, S., "Can black carbon in snow be detected by remote sensing?," *J. Geoph. Res.: Atmos.* **118**, 779–786 (2013).
[20] Zhang, Z., Zhou, L., and Zhang, M., "A progress review of black carbon deposition in Arctic snow and ice and its impact on climate change," *Adv. Polar Sci.* **35**(2), 178–191 (2024).
[21] Niittynen, P., Heikkinen, R., and Luoto, M., "Snow cover is a neglected driver of Arctic biodiversity loss," *Nat. Clim. Change* **8**, 997–1003 (2018).
[22] Réveillet, M., Dumont, M., Gascoin, S., Lafaysse, M., Nabat, P., Ribes, A., Nheili, R., Tuzet, F., Ménégoz, M., Morin, S., Picard, G., and Ginoux, P., "Black carbon and dust alter the response of mountain snow cover under climate change," *Nat. Comun.* **13**, 5279:1–12 (2022).
[23] Gilardoni, S., Vignati, E., and Wilson, J., "Using measurements for evaluation of black carbon modeling," *Atmos. Chem. Phys.* **11**, 439–455 (2011).
[24] Thomas, J., Polashenski, C., Soja, A., Marelle, L., Casey, K., Choi, H., Raut, J., Wiedinmyer, C., Emmons, L., Fast, J., Pelon, J., Law, K., Flanner, M., and Dibb, J., "Quantifying black carbon deposition over the Greenland ice sheet from forest fires in Canada," *Geophys. Res. Lett.* **44**, 7965–7974 (2017).
[25] Schwarz, J., Gao, R., Perring, A., Spackman, J., and Fahey, D., "Black carbon aerosol size in snow," *Sci. Rep.* **3**, 1356:1–5 (2013).
[26] Walker, D., Halfpenny, J., Walker, M., and Wessman, C., "Long-term studies of snow-vegetation interactions," *BioScience* **43**(25), 287–301 (1993).
[27] Bond, T. and Bergstrom, R., "Light absorption by carbonaceous particles: An investigative review," *Aerosol Sci. Tech.* **40**, 27–67 (2006).

[28] Kirchstetter, T., Novakov, T., and Hobbs, P., "Evidence that the spectral dependence of light absorption by aerosols is affected by organic carbon," *J. Geophys. Res.* **109**(D21208), 1–12 (2004).
[29] Olson, M., Garcia, M., Robinson, M., Rooy, P., Dietenberger, M., Bergin, M., and Schauer, J., "Investigation of black and brown carbon multiple-wavelength-dependent light absorption from biomass and fossil fuel combustion source emissions," *J. Geophys. Res. Atmos.* **120**, 6682–6697 (2015).
[30] Ramachandran, S. and Rajesh, T., "Black carbon aerosol mass concentrations over Ahmedabad, an urban location in Western India: Comparison with urban sites in Asia, Europe, Canada, and the United States," *J. Geophys. Res.* **112**(D06211), 1–19 (2007).
[31] Olson, M., Yuqin, W., de Foy, B., Li, Z., Bergin, M., Zhang, Y., and Schauer, J., "Source attribution of black and brown carbon near-UV light absorption in Beijing, China and the impact of regional air-mass transport," *Sci. Total Environ.* **807**, 150871:1–11 (2022).
[32] Pons, T., "Seed responses to light," in [*Seeds: The ecology of regeneration in plant communities*], Fenner, M., ed., 237–260, CABI Publishing, Wallingford, UK (2000).
[33] Smith, H., "Light quality, photoperception, and plant strategy," *Ann. Rev. Plant Physiol.* **33**, 481–518 (1982).
[34] Richardson, S. and Salisbury, F., "Plant responses to light penetrating snow," *Ecology* **58**(5), 1152–1158 (1977).
[35] Curl Jr., H., Hardy, J., and Ellermeier, R., "Spectral absorption of solar radiation in Alpine snowfields," *Ecology* **53**(6), 1189–1194 (1972).
[36] Gerland, S., Winther, J., Øbaek, J., Liston, G., Øristland, N., Blanco, A., and Ivanov, B., "Physical and optical properties of snow covering Artic tundra and Svalbard," *Hydrol. Processes* **13**, 2331–2343 (1999).
[37] Mølmann, J., Dalmannsdottir, S., Hykkerud, A., Hytönen, T., Samkumar, A., and Jaakola, L., "Influence of Arctic light conditions on crop production and quality," *Physiol. Plantarum* **172**, 1931–1940 (2021).
[38] Shumilov, O., Kasatkina, E., and Potorochin, E., "Solar and climate factors affecting tree-ring growth of mountain birch (*betula pubescens*) beyond the Northern timberline on Kola Peninsula, Northwestern Russia," *Forests* **15**, 37:1–13 (2024).
[39] Lüttge, U. and Hertel, B., "Diurnal and annual rhythms in tress," *Trees* **23**, 683–700 (2009).
[40] Benomar, L., Lamhamedi, M., and Rainville, A., "Variation in bud set process among eight genetically improved white spruce seed sources from Eastern Canada," *Tree Planters' Notes* **63**(1), 51–60 (2020).
[41] Cooke, J., Eriksson, M., and Juntilla, O., "The dynamic nature of bud dormancy in trees: Environmental control and molecular mechanisms," *Plant Cell Physiol.* **35**(10), 1707–1728 (2012).
[42] Warren, S., "Optical properties of ice and snow," *Philos. T. Roy. Soc. A* **377**, 20180161:1–17 (2019).
[43] Kou, L., *Black carbon: Atmospheric measurements and radiative effect*, PhD thesis, Dalhousie University, Halifax, Nova Scotia, Canada (October 1996).
[44] Kang, S., Zhang, Y., Qian, Y., and Wang, H., "A review of black carbon in snow and ice and its impact on the cryosphere," *Earth-Sci. Rev.* **210**, 103346:1–12 (2020).
[45] Varsa, P., Baranoski, G., and Kimmel, B., "SPLITSnow: A spectral light transport model for snow," *Remote Sens. Environ.* **255**, 112272:1–20 (2021).
[46] Varsa, P., *A First-Principles Framework for Simulating Light and Snow Interactions*, PhD thesis, University of Waterloo, Waterloo, Ontario, Canada (March 2025).
[47] Allen, W., Gausman, H., Richardson, A., and Thomas, J., "Interaction of isotropic light with a compact plant leaf," *J. Opt. Soc. Am.* **59**(10), 1376–1379 (1969).
[48] Baranoski, G. and Rokne, J., [*Light Interaction with Plants: A Computer Graphics Perspective*], Horwood Publishing, Chichester, UK (2004).
[49] Warren, S. and Brandt, R., "Optical constants of ice from the ultraviolet to the microwave: A revised compilation," *J. Geoph. Res. Atmos.* **113**(D14), D14220:1–10 (2008).
[50] Palmer, K. and Williams, D., "Optical properties of water in the near infrared," *J. Opt. Soc. Am.* **64**(8), 1107–1110 (1974).
[51] Pope, R. and Fry, E., "Absorption spectrum (380–700 nm) of pure water. II. Integrating cavity measurements," *Appl. Optics* **36**(33), 8710–8723 (1997).

[52] Jennings, S. and Pinnick, R., "Relationships between visible extinction, absorption and mass concentration of carbonaceous smokes," *Atmos. Environ.* **14**, 1123–1129 (1980).
[53] Park, K., Chow, J., Watson, J., Trimble, D., Doraiswamy, P., Park, K., Arnott, W., Stroud, K., Bowers, K., Bods, R., Petzold, A., and Hansen, A., "Comparison of continuous and filter-based carbon measurements at the Fresno supersite," *Air & Waste Manage. Assoc.* **56**, 474–491 (2006).
[54] Briggs, N. and Long, C., "Critical review of black carbon and elemental carbon source apportionment in Europe and the United States," *Atmos. Environ.* **144**, 409–427 (2016).
[55] Ramachandran, S. and Kedia, S., "Black carbon aerosols over an urban region: Radiative forcing and climate impact," *J. Geophys. Res.* **115**(D10202), 1–11 (2010).
[56] Fierz, C., Armstrong, R., Durand, Y., Etchevers, P., Greene, E., McClung, D., Nishimura, K., Satyawali, P., S., and Sokratov, S., "The international classification for seasonal snow on the ground," Tech. Rep. IHP-VII Technical Documents in Hydrology N°83, IACS Contribution N°1, International Hydrological Programme of the United Nations Educations, Scientific and Cultural Organization, UNESCO-IHP, Paris, France (2009).
[57] Salvatori, R., Salzano, R., Valt, M., Cerrato, R., and Ghergo, S., "The collection of hyperspectral measurements on snow and ice covers in Polar regions (SISpec 2.0)," *Remote Sens.* **14**, 2213:1–14 (2022).
[58] Weingartner, E., Saathoff, H., Schnaiter, M., Streit, N., Bitnar, B., and Baltensperger, U., "Absorption of light by soot particles: Determination of absorption coefficient by means of aethalometers," *J. Aerosol Sci.* **34**, 1445–1463 (2003).
[59] Liu, Q., Ma, T., Olson, M., Liu, Y., Zhang, T., Wu, Y., and Schauer, J., "Temporal variations of black carbon during haze and non-haze days in Beijing," *Sci. Rep.* **6**, 33331:1–10 (2016).
[60] Dumont, M., Brissaud, O., Picard, G., Schmitt, B., Gallet, J.-C., and Arnaud, Y., "High-accuracy measurements of snow bidirectional reflectance distribution function at visible and NIR wavelengths – comparison with modelling results," *Atmos. Chem. Phys.* **10**(5), 2507–2520 (2010).
[61] Mekhontsev, S., Prokhorov, A., and Hanssen, L., "Experimental characterization of blackbody radiation sources," in [*Radiometric Temperature Measurements II. Applications*], Zhang, Z., Tsai, B., and Machin, G., eds., 57–136, Elsevier, Oxford, UK (2010).
[62] Baranoski, G., Chen, B. K. T., and Miranda, E., "Assessing the spectral sensitivity of Martian terrains to iron oxide variations using the SPLITS model," *IEEE J-STARS* **8**(7), 3404–3413 (2015).
[63] Gross, D., "Report from the fidelity implementation study group," in [*Simulation Interoperability Workshop, Simulation Interoperability and Standards Organization*], (1999). Paper 99S-SIW-167.
[64] Vance, T., Huang, T., and Butler, K., "Big data in Earth science: Emerging practice and promise," *Science* **383**(6688), 1193:1–7 (2024).
[65] Varsa, P. and Baranoski, G., "*In silico* assessment of light penetration into snow: Implications to the prediction of slab failures leading to avalanches," in [*Proc. of SPIE Vol. 11863, Earth Resources and Environmental Remote Sensing/GIS Applications XII*], Schulz, K., ed., **11863**, 1186305:1–10 (2021).
[66] Varsa, P. and Baranoski, G., "On the sensitivity of snow bidirectional reflectance to variations in grain characteristics," in [*Proc. of SPIE Vol. 11856, Remote Sensing for Agriculture, Ecosystems, and Hydrology XXIII*], Neale, C. and Maltese, A., eds., 118560G:1–10 (2021).
[67] Natural Phenomena Simulation Group, *Run SPLITSnow Online.* School of Computer Science, University of Waterloo, Ontario, Canada (2021). Link to access model interface: http://www.npsg.uwaterloo.ca/models/splitsnow-i.php.
[68] Baranoski, G., Dimson, T., Chen, T., Kimmel, B., Yim, D., and Miranda, E., "Rapid dissemination of light transport models on the web," *IEEE Comput. Graph.* **32**(3), 10–15 (2012).
[69] Natural Phenomena Simulation Group, *Snow Data.* School of Computer Science, University of Waterloo, Ontario, Canada (2020). http://www.npsg.uwaterloo.ca/data/snow.php.
[70] Hamby, D., "A review of techniques for parameter sensitivity analysis of environmental models," *Environ. Monit. Assess.* **32**, 135–154 (1994).
[71] Hamby, D., "A comparison of sensitivity analysis techniques," *Health Phys.* **68**, 195–204 (1995).
[72] Hoffman, F. and Gardner, R., "Evaluation of uncertainties in radiological assessment models," in [*Radiological Assessment: A Textbook on Environmental Dose Analysis*], Till, J. and Meyer, H., eds., 1–55, Division of Systems Integration, Office of Nuclear Reactor Regulation, U.S. Nuclear Regulatory Commision, NRC FIN B0766, Washington, DC, USA (1983). Chapter 11.

[73] Brandt, R., Warren, S., and Clarke, A., "A controlled snowmaking experiment testing the relation between black carbon content and reduction of snow albedo," *J. Geoph. Res.* **118**, D08109:1–6 (2011).

[74] Flanner, M., Arnheim, J., Cook, J., Dang, C., He, C., Huang, X., Singh, D., Skiles, S., Whicker, C., and Zender, C., "SNICAR-ADv3: A community tool for modeling spectral snow albedo," *Geosci. Model Dev.* **14**, 7673–7704 (2021).

[75] Wiscombe, W. and Warren, S., "A model for the spectral albedo of snow. I: Pure snow," *J. Atmos. Sci.* **37**, 2712–2733 (1980).

[76] Robledano, A., Picard, G., Dumont, M., Flin, F., Arnaud, L., and Libois, Q., "Unraveling the optical shape of snow," *Nature Com.* **14**, 3955:1–11 (2023).

[77] Robson, T. and Aphalo, P., "Transmission of ultraviolet, visible and near-infrared radiation to plants within a seasonal snowpack," *Photochem. Photobiol. Sci.* **18**(1), 1963–1971 (2019).

[78] Kameniarová, M., Černý, M., Novák, J., Ondrisková, V., Hrušková, L., Berka, M., Vankova, R., and Brozbohatý, B., "Light quality modulates plant cold response and freezing tolerance," *Front. Plant Sci.* **13**, 886103:1–17 (2022).

[79] Ingrosso, G., Ceccarelli, C., Giglio, F., Giordano, P., Hefter, J., Langone, L., Miserocchi, S., Mollenhauer, G., Nogarotto, A., Sabino, M., and Tesi, T., "Greening of Svalbard in the twentieth century driven by sea loss and glaciers retreat," *Commun. Earth Environ.* **6**(30), 1–13 (2025).

[80] Lubenow, D. and Reinhardt, K., "The environmental drivers of annual variation in forest greenness are variable in the northern Intermountain West, USA," *Ecosphere* **11**(8), e03212:1–15 (2020).

[81] Arndt, K., Santos, M., Ustin, S., Davidson, S., Stow, D., Oechel, W., Tran, T., Graybill, B., and Zona, D., "Arctic greening associated with lengthening growing seasons in Northern Alaska," *Environ. Res. Lett.* **14**, 1250018:1–13 (2019).

[82] Barrere, M., Dominé, F., Belke-Brea, M., and Sarrazin, D., "Snowmelt events in autumn can reduce or cancel the soil warming effect of snow-vegetation interactions in the Arctic," *J. Climate* **31**, 9507–9518 (2018).

[83] Ciani, A., Goss, K., and Schwarzenbach, R., "Light penetration in soil and particulate materials," *Eur. J. Soil. Sci.* **56**, 561–574 (2005).

[84] Pettorelli, N., [*The Normalized Difference Vegetation Index*], Oxford University Press, Oxford, U.K. (2013).

[85] Riggs, G., Hall, D., and Salomonson, V., "A snow index for the Landsat thematic mapper and moderate resolution imaging spectroradiometer," in [*International Geoscience and Remote Sensing Symposium - IGARSS*], 1942–1944 (1994).

[86] Salzano, R. (Institute of Atmospheric Pollution Research, IIA National Research Council of Italy, CNR, Sesto Fiorentino, Florence, Italy), "Sispec snow & ice spectral library data access." Personal Communication (January 2023).